Graphene-based long period grating fiber sensor as detector of metallic impurities in composite materials

I. S. DONTU, D. SAVASTRU*, V. SAVU, D. TENCIU, A. STANCIU
National Institute R&D of Optoelectronics INOE 2000, 409 Atomistilor Str., Magurele, 077125, Ilfov, Romania

In this paper we report results on simulation of a fibre optic sensors class of potential interest for various chemical sensing applications, namely Long Period Grating Fibre Sensors (LPGFS) having a graphene layer deposited on the cladding in the grating zone. Studied LPGFS consists of single mode (SM) fused silica optical fibre onto/into which a grating with 10 µm to 1000 µm is inscribed over a 5 mm to 75 mm length zone. In this zone the PMMA protection layer is removed creating a direct contact of the optic fibre with the ambient medium. The sensing capabilities of LPGFS are greatly improved by deposition of a graphene (G) layer, a two-dimensional carbon material on this optic fibre cladding zone.

(Received April 2, 2025; accepted April 15, 2025)

Keywords: Composite material, Graphene layer, Long period grating fibre sensors (LPGFS)

1. Introduction

The increasing demand for high-performance composite materials in aerospace, automotive, and structural applications has necessitated advanced sensing techniques for detecting impurities that can compromise their integrity. Metallic impurities, even in trace amounts, can alter the electrical, thermal, and mechanical properties of composites, leading to potential failure in critical applications. Therefore, the development of highly sensitive and selective detection methods is crucial for ensuring material quality and reliability. For many applications in medicine, industry, chemistry, defense and research fields there is an increasing interest in graphene based complex composite materials structures. One inherent problem related to this type of composite materials is the presence of metallic or non-metallic impurities at the interface between the woven or non-woven and graphene layers. The impurity appears during the graphene fabrication process, the most significant being the Nickel and Oxygen ions [1, 2].

Graphene, with its exceptional electrical conductivity, optical transparency, and strong interaction with light, has emerged as a promising material for sensing applications. When integrated with fiber optic sensors, graphene enhances sensitivity and enables the detection of minute changes in the surrounding medium. In particular, graphene-based long-period grating (LPG) fiber sensors have attracted significant attention due to their high refractive index sensitivity, wide tunability, and compatibility with real-time monitoring applications [3-5].

Metallic impurities in composite materials, especially polymer matrix composites (PMCs), can detrimentally impact mechanical strength, thermal stability, and electrical conductivity. Detecting such contaminants at trace levels during the manufacturing process is essential for ensuring product reliability in critical sectors, including aerospace, automotive, and biomedical industries. Long period grating (LPG) fiber sensors exhibit refractive index sensitivity through coupling between core and cladding modes. The addition of a graphene layer to the grating region provides a highly reactive interface for metallic species, leading to measurable spectral shifts. Although experimental validations have shown promising results, detailed simulations are crucial to understanding the physical mechanisms and optimizing sensor designs [5 – 11].

The integrity of composite materials is vital in numerous advanced engineering applications. Metallic impurities, either as residuals from manufacturing processes or as byproducts of environmental exposure, can compromise composites by catalyzing degradation or altering conductive pathways. Conventional methods such as atomic absorption spectroscopy (AAS) or inductively coupled plasma mass spectrometry (ICP-MS) require complex sample preparation and are not suitable for real-time applications [6 -11].

Optical fiber sensors, especially long period gratings (LPGs), offer a promising alternative due to their compactness, immunity to electromagnetic interference, and multiplexing capabilities. Graphene, a two-dimensional material composed of a single layer of carbon atoms, exhibits remarkable optical absorption, high surface area, and strong affinity towards metallic ions via π-π interactions and charge transfer mechanisms. This work explores the integration of graphene with LPG fiber sensors to enhance sensitivity and selectivity towards metallic impurities in composites. The enhancement can be attributed to graphene's high surface adsorption capacity and its modulation of the cladding modes of the LPG. Metallic ions interact with graphene via coordination bonding and electron transfer, altering the local refractive index and increasing coupling strength between core and cladding modes [12 – 18].

This study presents a simulation-based approach to investigate the operation of a graphene-coated LPG fiber sensor for detecting metallic impurities in composite materials. By leveraging the unique optical properties of graphene and the resonant characteristics of LPG structures, the sensor can achieve high precision in impurity detection. The simulation explores the interaction of metallic nanoparticles with the evanescent field of the LPG structure, analyzing the shifts in resonance wavelengths as an indicator of contamination levels.

Through this simulation study, we aim to provide insights into the potential of graphene-based LPG fiber sensors as efficient and non-destructive tools for impurity detection. The findings could contribute to the advancement of smart sensing technologies for quality assurance in industrial composite fabrication.

2. Theory

A Long Period Grating (LPG) is a periodic modulation of the refractive index along the core of an optical fiber, typically with a grating period of hundreds of micrometers. LPGs couple the core mode to cladding modes at specific wavelengths, resulting in resonant dips in the transmission spectrum. The sensitivity of LPG sensors makes them suitable for measuring external refractive index, temperature, strain, and other parameters. Graphene, a two-dimensional material made up of carbon atoms in a hexagonal lattice, has unique optical, mechanical, and electrical properties:

- High optical absorption (in the near-infrared and visible range)
- High surface-to-volume ratio
- Tunable conductivity via chemical potential
- Strong interaction with evanescent fields

When integrated with LPG fiber sensors, graphene enhances sensitivity due to:

- Strong evanescent field interaction between the cladding mode and graphene layer.
- The modulation of the graphene's refractive index with environmental changes (e.g., gas adsorption, biomolecule binding) which perturbs the LPG resonance.

When graphene is coated on the fiber surface (typically over the grating region), it alters n_{clad}, due to its optical properties. Environmental changes (e.g., analyte binding, temperature shifts) influence graphene's surface conductivity and refractive index, leading to shifts in λres detectable as a wavelength shift in the transmission spectrum [19, 20].

The advantages of Graphene-Based LPG Sensors are:

- Enhanced sensitivity due to strong graphene-light interaction.
- Wide range of sensing applications, including biochemical sensing, gas detection, and humidity monitoring.
- Multiparameter sensing by tuning graphene properties (chemical doping, layer number).
- Improved selectivity when functionalized graphene is used (e.g., with antibodies, enzymes).

The mathematical model for LPG typically uses Coupled Mode Theory (CMT), which describes how light couples from the core mode to the cladding mode [21-23].

The basic equations are:

$$\frac{dA_c}{dz} = -jkA_{cl}e^{j\Delta\beta z} \tag{1}$$

$$\frac{dA_{cl}}{dz} = -jkA_c e^{j\Delta\beta z} \tag{2}$$

where:

- A_c and A_{cl} are the amplitudes of the core and cladding modes.
- κ is the coupling coefficient (depends on index modulation and overlap of mode fields).
- $\Delta\beta=\beta c-\beta cl-2\pi/\Lambda$
- Λ is the grating period.

The resonance wavelength λ_{res} is given when $\Delta\beta=0$:

$$\beta_c(\lambda_{res}) - \beta_{cl}(\lambda_{res}) = \frac{2\pi}{\Lambda} \tag{3}$$

where β_c and β_{cl} are the propagation constants of the core and cladding modes.

When a thin layer of graphene is deposited on the cladding, it affects the effective refractive index of the cladding modes due to: graphene's optical conductivity, surface plasmon polariton (SPP) effect in the mid-IR to THz range and electro-refractive tuning (via graphene's chemical potential.

Graphene Optical Conductivity is given by Kubo Formula:

$$\sigma_g(\omega) = \sigma_{intra}(\omega) + \sigma_{inter}(\omega) \tag{4}$$

Graphene introduces a surface impedance $Z_g=1/\sigma_g$, which modifies the boundary conditions at the cladding interface, changing the effective refractive index $n_{eff,cl}$ of cladding modes:

$$n'_{eff,cl} = n_{eff,cl} + \delta n_g \tag{5}$$

where δn_g depends on graphene's σ_g and thickness t_g (typically monolayer or few layers).

The sensitivity of the LPG sensor is often defined as:

$$S = \frac{d\lambda_{res}}{dn_{ext}} \tag{6}$$

where n_{ext} is the external refractive index (e.g., surrounding medium). Graphene increases S because it enhances the interaction between the cladding mode and the external environment due to its plasmonic and tunable properties.

The transmission through the LPG is given by:

$$T(\lambda) = 1 - \left| \frac{kL}{\sqrt{k^2+(\Delta\beta/2)^2}} \sin(\sqrt{k^2 + (\Delta\beta/2)^2} L \right| \quad (7)$$

where *L* is the grating length.

A Graphene-Based LPG Fiber Sensor is composed from an optical fiber core that is the central region where light propagates; a grating region: a section of the fiber where periodic refractive index modulation (LPG) is written; a cladding: surrounds the core and supports cladding modes; a graphene layer which is a thin coating (usually a monolayer or few-layer graphene) on the outer surface of the fiber over the LPG region; an evanescent field: part of the cladding mode that extends into the graphene layer, enabling interaction, and an incident light & transmission spectrum: a broadband light source inputs light into the fiber, and resonant dips appear in the transmission spectrum due to cladding mode coupling [25].

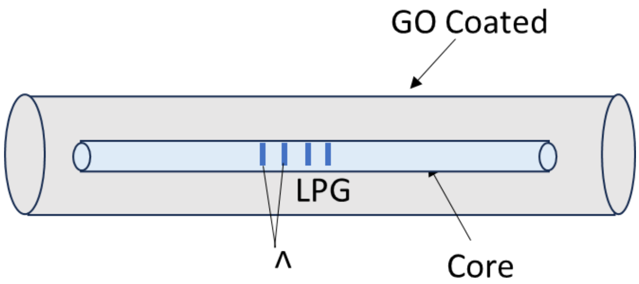

Fig. 1. The Graphene-Based LPG Fiber Sensor diagram

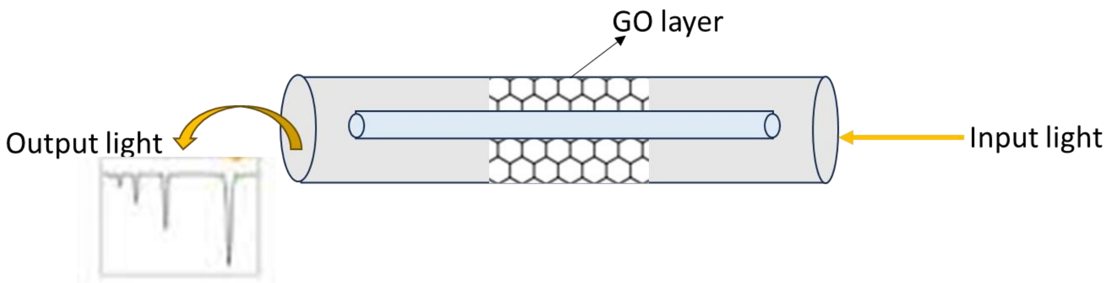

Fig. 2. Schematic view of the optical transducer based on LPG with GO (colour online)

Graphene oxide is a chemically modified graphene that is typically prepared by oxidation and exfoliation of graphite-bearing oxygen functional groups, such as carboxyl (-COOH), hydroxyl (-OH), or epoxy (-O-), on their basal planes and edges with the modified Hummers' method [26].

3. Simulation results

In this paper we report results on simulation of a fibre optic sensors class of potential interest for various chemical sensing applications, namely Long Period Grating Fibre Sensors (LPGFS) having a graphene layer deposited on the cladding in the grating zone. Studied LPGFS consists of single mode (SM) fused silica optical fibre onto/into which a grating with 10 µm to 1000 µm is inscribed over a 5 mm to 75 mm length zone. In this zone the PMMA protection layer is removed creating a direct contact of the optic fibre with the ambient medium. The sensing capabilities of LPGFS are greatly improved by deposition of a graphene (G) layer, a two-dimensional carbon material on this optic fibre cladding zone. The G layer acts as a refractive index matching between the optic fibre and the ambient medium, increasing the sensitivity of the optic sensor. During the simulations, the main issue of interest is the displacement of peak wavelengths and bandwidths broadening of the absorption bands corresponding to the energy transfer from core propagating mode to the possible cladding modes at the interaction with the grating as results of ambient medium different factors action. The ambient medium is the graphene layer of a composite material. The sensor can be also placed at the interface between the woven or non-woven and graphene layers. During the simulations a special care was dedicated to investing the role of graphene layer thickness from one-atom-thickness up to 400 nm. There were analyzed the cases of the three main types of graphene commercially available, namely graphene (G), graphene oxide (GO) and reduced graphene oxide (rGO). The detection of chemical impurities is accomplished by measuring the modification of graphene optical properties or the induced stress.

In Fig. 3 is shows a slow and steady increase in λ_{res} variation for lower values of n_{am}. As n_{am} approaches 1.5, there is a sharp exponential increase in λ_{res} variation. The variation remains nearly zero for most of the range (approximately between 1.0 and 1.3). A rapid rise occurs beyond $n_{am} \approx 1.4$ reaching a high value near 150 nm. The behavior suggests a threshold effect where a small change in n_{am} beyond a critical point results in a dramatic shift in resonance wavelength. This could indicate a strong sensitivity of the LPG (Long-Period Grating) to refractive index changes in this range. The sharp sensitivity at higher values of n_{am} suggests this system could be useful for sensing applications where detecting minute changes in refractive index is crucial. Optical fiber sensors might leverage this property to detect environmental changes in gas or liquid compositions.

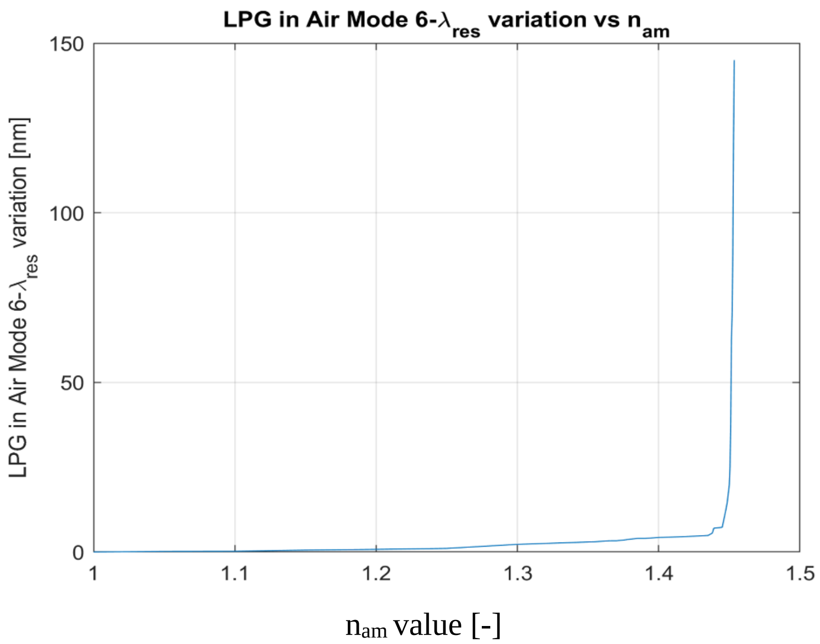

Fig. 3. Variation of the resonance wavelength of LPG in Air Mode 6 as a function of n_{am} (likely the ambient refractive index) (colour online)

Long-period gratings (LPGs) are optical fiber structures that couple light from the core mode to co-propagating cladding modes, leading to attenuation at specific resonance wavelengths (λ_{res}). These resonances are highly sensitive to changes in external refractive index (n_{am}), making LPGs excellent for sensing applications. The resonance wavelength λres of an LPG is determined by the phase-matching condition:

$$\lambda_{res}=\Lambda(n_{eff,core} - n_{eff,clad})$$

where:

- Λ is the grating period,
- $n_{eff,coren}$ and $n_{eff,clad}$ are the effective refractive indices of the core and cladding modes, respectively.

As the external refractive index (n_{am}) increases, it affects the cladding mode's effective index ($n_{eff,clad}$), causing a shift in λ_{res}. From the graph, λ_{res} remains nearly constant for lower n_{am} values but exhibits an exponential rise near $n_{am} \approx 1.4$. This can be explained by the following: weak sensitivity at low n_{am}; when n_{am} is much lower than the cladding index, the cladding modes are well-confined, and their effective indices remain stable, small variations in n_{am} do not significantly alter $n_{eff,clad}$, resulting in minimal λ_{res} shifts. In Transition Region (~n_{am}=1.3 to 1.41) n_{am} approaches the cladding refractive index, the cladding modes start leaking into the surrounding medium, altering $n_{eff,clad}$ more drastically.

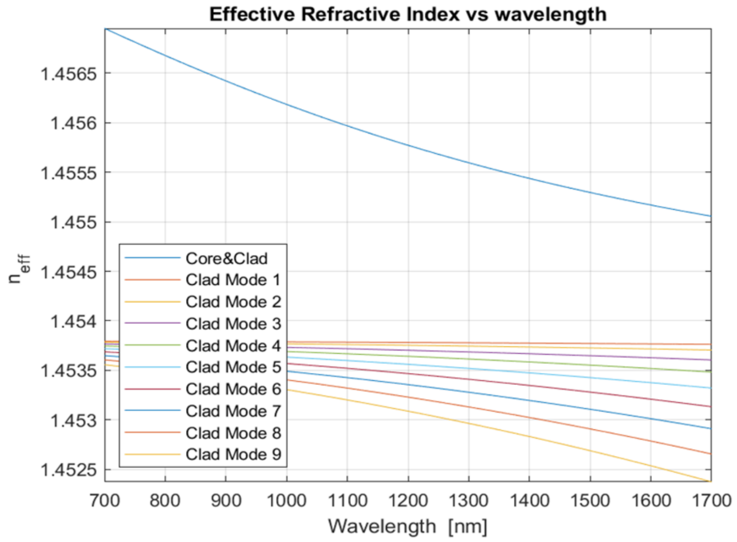

Fig. 4. Effective refractive index vs wavelength simulated for LPGFS (colour online)

This transition leads to increased sensitivity in λ_{res} variation. In Critical Region ($\sim n_{am} \approx 1.45$) n_{am} approaches the cladding index, total internal reflection at the cladding boundary weakens, and the cladding modes become highly sensitive. A small change in n_{am} causes a large change in $n_{eff,clad}$ resulting in an exponential shift in λ_{res}.

LPGFS simulation is accomplished by numerical methods starting from Electromagnetic Field (EM) equations for propagation through optical fiber and is accomplished in 3 stages.

STAGE 1 consists of effective values of refractive index of EM propagation modes calculation.

The results obtained for Core & Cladding (first 9 possible) modes are presented in the Fig. 4. The effective refractive index of the core mode decreases as the wavelength increases. This behavior follows the typical dispersion relation in optical fibers, where the core's effective refractive index decreases with increasing wavelength. The cladding modes have lower effective refractive indices than the core mode. The cladding mode indices show slight variation with wavelength but are more stable compared to the core. Higher-order cladding modes tend to exhibit a more noticeable dispersion effect. There is a clear gap between the core mode index and the cladding mode indices, which is essential for guiding light in the core. This gap influences the coupling conditions in Long-Period Gratings (LPGs) since phase-matching conditions depend on these values. Since the core index decreases more significantly than the cladding indices, the phase-matching condition shifts accordingly. This effect contributes to the wavelength sensitivity of LPG-based sensors and tunable optical filters. Small variations in external refractive index can alter the cladding mode properties, affecting the resonance wavelength. Understanding n_{eff} variation helps in designing filters and gratings for optical communication systems. The separation between the core and cladding indices determines the strength of coupling in LPGs, affecting their efficiency and response time.

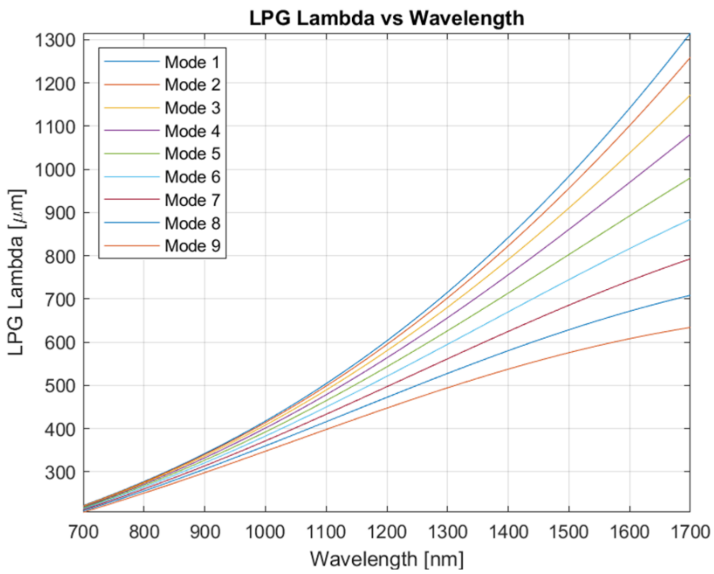

Fig. 5. Phase matching curves (PMC) (colour online)

Next step in LPGFS simulation consists of Phase Matching Curves (PMC).

PMC are parametric curves formed by pairs (wavelength – grating period) for which the Bragg resonance condition is fulfilled. Bragg resonance condition is the maximum energy transfer from the core mode to the clad-ding modes when interacting with the grating. The curves show an increasing trend, meaning that as the wavelength increases, the LPG Lambda also increases. The increase appears to be nonlinear, with the slope becoming steeper at higher wavelengths. The graph includes nine different modes (Mode 1 to Mode 9), each represented by a different color. These modes exhibit similar trends but differ in their values, with higher modes having higher LPG Lambda values. Each mode follows a distinct trajectory, indicating a mode-dependent response in the LPG Lambda. The separation between modes increases at higher wavelengths, meaning higher-order modes diverge more significantly.

This graph likely represents Long Period Grating (LPG) properties in optical fibers, where LPG Lambda corresponds to the grating period required for coupling different propagating modes in an optical fiber.

The nonlinear trend suggests dispersion effects, where the LPG response varies with wavelength.

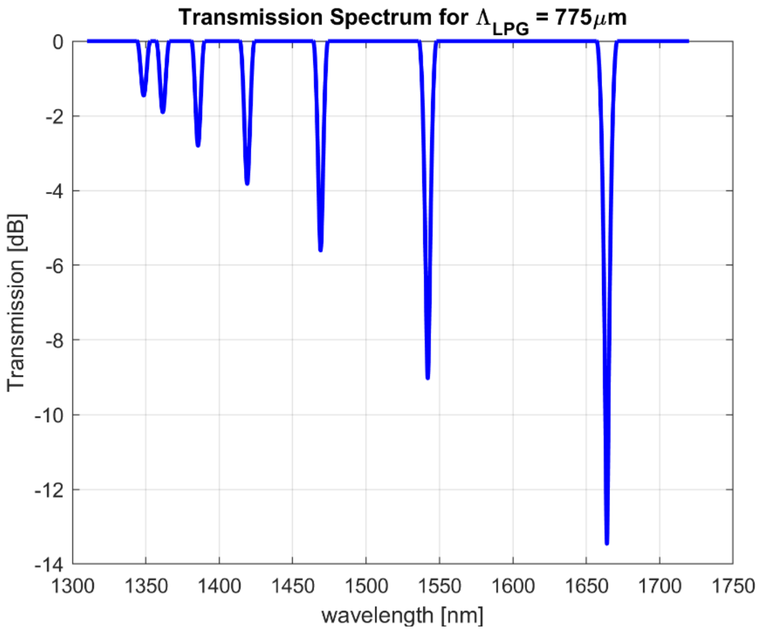

Fig 6. Transmission spectrum calculation on the basis of PMC (colour online)

STAGE 2 of LPGFS simulation consists of transmission spectrum calculation on the basis of PMC.

LPGFS transmission spectrum is composed of absorption bands with peak wavelengths situated at grating Bragg resonance wavelengths. In the graph 6 are presented the results calculated for a grating with 50 mm length and 775 mm grating period. The LPGFS use is based on determining the spectral shifts of the absorption spectra when ambient refractive index changes. The spectrum ranges from 1300 nm to 1750 nm. This suggests that the optical device operates in the near-infrared (NIR) region. The transmission values are mostly near 0 dB, except for dips. Negative dB values indicate the attenuation at specific wavelengths. The spectrum has multiple sharp resonance dips at various wavelengths. These dips correspond to wavelengths where light is coupled to cladding modes, causing attenuation. The most significant dip appears around 1650 nm, reaching approximately -14 dB. This is a characteristic long-period fiber grating (LPG) spectrum, used for applications such as optical sensing, telecommunications, and wavelength filtering.

The positions and depths of the dips depend on parameters like refractive index, grating period, and environmental factors (e.g., temperature, strain, and surrounding medium).

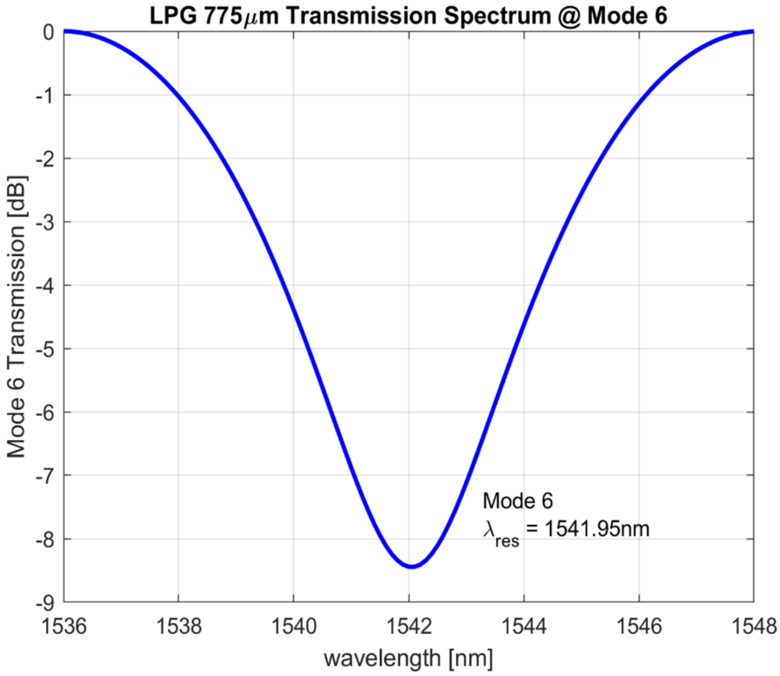

Fig. 7. Transmission spectrum of a Long Period Grating (LPG) with a period of 775 μm at Mode 6 (colour online)

Fig. 7 presents the transmission spectrum of Mode 6. Its peak Bragg resonance wavelength is situated at λ_{res} = 1541.95 nm. Mode 6 was chosen because its λ_{res} is placed near the middle of the LPGFS interrogator input spectral domain.

The Mode 6 spectral shift appears as a result of bending or stress induced by composite strain. The curve is symmetric and V-shaped, indicating a resonance dip. The lowest point of the curve represents the resonant wavelength (λ_{res}), which is 1541.95 nm. The transmission decreases as it approaches this resonance and reaches a minimum at the resonance before increasing again. The resonance dip occurs due to mode coupling in the fiber grating, where a particular mode (Mode 6 in this case) undergoes coupling at the given wavelength. The deeper the dip, the stronger the coupling between the core and cladding modes in the LPG. The position of this dip can shift with changes in temperature, strain, or refractive index, making LPGs useful in sensing applications. The resonant wavelength is 1541.95 nm, as annotated on the graph. The maximum transmission loss at resonance is about -8.5 dB. The spectral shape is typical for LPG transmission spectra, with a smooth attenuation profile.

4. Conclusions

This study presents a detailed simulation of a graphene-based LPG fiber sensor designed for detecting metallic impurities in composite materials. Results confirm that the integration of graphene significantly enhances sensor sensitivity by improving the interaction between the evanescent field and adsorbed metallic species. The simulation findings serve as a valuable foundation for the optimization of sensor parameters and pave the way for experimental validation and industrial implementation.

The presented results are obtained using a finite-element method simulation model. The presented results of simulations are thought as a tool for Long Period Grating Fiber Sensors detectors function of the materials, parts and devices available for the designers

Acknowledgements

This research was funded by the Romanian National Research Authority, Ministry of Education and Research, and the Ministry grant number OPTRONICA VII PN23 05 (11N/2023).

References

[1] C. Soutis, Prog Aerosp Sci. **41**(2), 143 (2005).
[2] D. Savastru, V. Savu, M. Rusu, M. Tautan, A. Stanciu, J. Optoelectron. Adv. M. **26**(7-8), 316 (2024).
[3] M. Rusu, D. Savastru, V. Savu, Al. Stanciu, M. Tautan, U.P.B. Sci. Bull. Series A **86**(4), 159 (2024).
[4] D. Savastru, S. Miclos, R. Savastru, I. Lancranjan, Composite Structures **183**, 682 (2018).
[5] S. Miclos, D. Savastru, R. Savastru, I. Lancranjan Composite Structures **183**, 521 (2018).
[6] T. Erdogan, IEEE Journal of Lightwave Technology **15**(8), 1277 (1997).
[7] P. Zhang, Y. Chen, Y. Li, Y. Zhang, J. Zhang, L. Huang, Sensors **20**, 2901, (2020)
[8] Bing Xu, Jun Huang, Liyun Ding, Jun Cai, Materials

Science & Engineering C, **107**, 110329, (2020)
[9] F. H. Koppens T. Mueller, Ph. Avouris, A. C. Ferrari, M. S. Vitiello, M. Polini, Nature Nanotechnology **9**(10), 780 (2014).
[10] COMSOL Multiphysics® User Guide (2024). COMSOL AB.
[11] M. I. Rusu, Y. Addab, C. Martin, C. Pardanaud, V. Savu, I. I. Lancranjan, D. Tenciu, Optoelectron. Adv. Mat. **17**(3-4), 159 (2023).
[12] K. S. Novoselov A. K. Geim , S. V. Morozov, D. Jiang, Y. Zhang, S. V. Dubonos, I. V. Grigorieva, A. A. Firsov, Science **306**(5696), 666 (2004)
[13] A. Zitoun, D. Fakis, N. Jayasree, S. Omairey, F. Oikonomidis, Z. Stoeva, M. Kazilas, SN Applied Sciences, **4**(58), (2022)
[14] A. K. Geim, K. S. Novoselov, Nature Materials **6**(3), 183 (2007).
[15] Y. Sharma, S. Kalra, R. Zafar, Ritambhara, Optoelectron. Adv. Mat. **17**(3-4), 112 (2023).
[16] K. Gurpreet, S. Rajandeep, S. Aaradhya, K. Harmanpreet, Optoelectron. Adv. Mat. **17**(5-6), 219 (2023).
[17] M. Hernaez, C. R. Zamarreño, S. Melendi-Espina, L. R. Bird, A. G. M. Francisco J. Arregui, Sensors, **17**,155 (2017)
[18] Yong Zha, Xue-gang Lia, Xue Zhoua, Ya-Nan Zhanga, Sensors and Actuators B: Chemical, **231**, 324 (2016)
[19] F. Esposito, L. Sansone, A. Srivastava, F. Baldini, S. Campopiano, F. Chiavaioli, M. Giordano, A. Giannetti, A. Iadicicco, Biosensors and Bioelectronics **172**, 112747, (2021).
[20] A. Popescu, D. Savastru, Al. Stanciu, J. Optoelectron. Adv. M. **26**(7-8), 264 (2024)
[21] https://en.wikipedia.org/wiki/Coupled_mode_theory
[22] Long Jin, Wei Jin, Jian Ju, and Yiping Wang, Journal of Lightwave Technology **28** (12), 1745 (2010)
[23] S. Miclos, D. Savastru, R. Savastru, I. I. Lancranjan, Composite Structure **218**, 15 (2019).
[24] I. Lancranjan, Dan Savastru, S. Miclos, J. Optoelectron. Adv. M **12**(8), 1636 (2010).
[25] M. Singh, S. Raghuwanshi, O. Prakash, IEEE Photonics Technology Letters **31**(17), 1473 (2019).
[26] W. S. Hummers, R. E. Offeman, Journal of the American Chemical Society **80**, 1339 (1958);

*Corresponding author: dsavas@inoe.ro